ARTICLES

Direct Cross-Linking of C_{70} in Ar Plasma

Masafumi Ata,* Ken'ichi Kurihara, and Noboru Takahashi

Hodogaya Laboratory, Research Institute of Innovative Technology for the Earth, Sony Corporation Research Center, 174 Fujitsuka-cho, Hodogaya-ku, Yokohama 240, Japan

Received: March 4, 1996; In Final Form: September 4, 1996[⊗]

C_{70} polymer films were prepared by rf plasma irradiation in Ar atmosphere. Laser desorption ionization time-of-flight mass spectra (LDITOF-MS) for the polymer films showed that C_2 loss occurred in the course of direct cross-linking of C_{70} molecules. The polymer structure is discussed based on molecular orbital (MO) calculations of C_{70} dimers at semiempirical levels, and the lower probability of direct cross-linking of C_{70} molecules than that of C_{60} molecules is suggested. The electric dark current of the plasma-polymerized C_{70} was 10^{-13} S/cm, compared to 10^{-8} S/cm in the C_{60} polymer prepared at the same plasma power. The almost-insulating electric conductivity of the C_{70} polymer is attributable to the lower probability of conductive cross-linking of C_{70} molecules originating from the electronic structure of C_{70}. The experimental and theoretical results suggest that the C_{70} molecule is the smallest carbon nanotube with polyhedral caps and that the chemical properties of the caps closely resemble the C_{60} molecule.

Introduction

Discovery of buckministerfullerene (C_{60})[1] and a novel method for preparing macroscopic amounts of fullerenes[2] has led to a significant volume of research on its unique physical and chemical properties. Polymers of C_{60} have been obtained by direct photochemical cross-linking of C_{60} molecules.[3] For the photoinduced C_{60} polymer, the mechanism for the photopolymerization of solid C_{60},[4] the kinetics of the photodimerization process,[5] photoelectron spectroscopy,[6] and Raman spectra[7] have been reported. Odd-numbered carbon clusters derived from C_{60} in an oxygenated atmosphere have been reported by McElvany *et al.*[8] Recently, linear polymer of C_{60} was confirmed in K- and Rb-doped C_{60} crystal.[9] Iwasa et al.[10] reported a phase transition of C_{60} crystal at high pressure and proposed a novel two-dimensional C_{60} polymer,[11] whose properties were theoretically examined.[12]

To obtain C_{60} polymer, we have adopted a plasma-polymerization technique.[13] The electric dark current of the polymer films was ca. 10^{-8} S/cm in ambient atmosphere, and a semiconductor-type temperature dependence of the conductivity at high temperatures domain was observed, suggesting a bandgap energy of 2.1 eV.[13] On the basis of MO calculations we proposed that the 1,2-C_{60} dimer molecule by [2+2]-cycloaddition was found to be the most plausible structure of a C_{60} dimer with intact C_{60} cages.[14] Similar theoretical results have been reported by several groups.[15] To further clarify the polymer structure, LDITOF and field desorption mass spectra of plasma-polymerized C_{60} films were measured and the dimer peaks were assigned with the aid of MO calculations.[16] There is evidence that four carbon atoms are frequently eliminated in the cross-linking of two C_{60} molecules. The most intense peak in the dimer mass range was therefore assigned to a C_{116} molecule with D_{2h} symmetry.[16]

Whereas many derivatives of C_{60} have been investigated, only a few derivatives of C_{70},[17] metal complexes of C_{70},[18] alkylated C_{70},[19] and hydrated and halogenated C_{70}[20] have been isolated and characterized. Photopolymerization of C_{70} was examined by Rao et al.[21] Their findings indicated that the molecule is less active than C_{60} toward cycloaddition.

In this article, we report the plasma polymerization of C_{70} in an Ar atmosphere. Raman spectra of polymer films of C_{70} are compared with the spectra of the pure C_{70} cage[22] and amorphous carbon films.[23] Furthermore, LDITOF mass analyses of the C_{70} polymer films are reported. Based on these observations and MO calculations at semiempirical levels, the structure of the polymer and the polymerization process as well as the mechanism under Ar plasma irradiation are discussed. Finally, the polymerization process of C_{70} is compared with that of C_{60}, and the characteristics of C_{70} polymers are presented.

Experimental Section

The C_{70} sample was purified using an activated aluminum column 200 cm long, with a *n*-hexane:toluene 9:1 v/v solution. The C_{70} sample was sealed in an evacuated glass tube after being heated for 12 h at 300 °C, and the sample was then crystallized using an electric heater equipped with two heating probes, which were set at 590 and 500 °C. The preparation of the plasma-polymerized C_{70} films was carried out in an Ar plasma at a power of 50 W. The other experimental details of plasma polymerization were identical to those reported previously.[13]

LDITOF-MS observations were carried out using JEOL LDI-1700 and Finnigan MAT Vision 2000 mass monitors, and both sets of apparatus were equipped with a N_2 laser. Mass monitoring of the plasma-polymerized C_{70} films was carried out without any matrix molecule for the reasons stated previously.[16] To compare the probability of direct cross-linking of C_{60} and C_{70} by UV irradiation, samples of C_{60}, C_{70}, and a 1:1 mixture of C_{60}/C_{70} were set on ionization targets, and the polymer peaks were observed. During the observation, the laser power was increased sufficiently to cause photopolymerization.

An Ar^+ laser (514.5 nm) used for excitation in Raman observation was operated at 20 mW and the beam spot was 1

[⊗] Abstract published in *Advance ACS Abstracts,* December 15, 1996.

S1089-5647(96)00664-5 CCC: $14.00

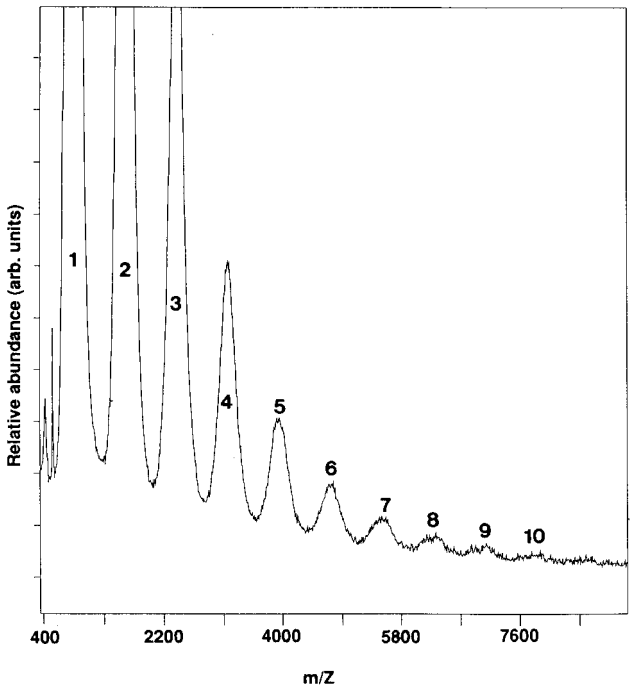

Figure 1. LDITOF-MS of a plasma-polymerized C_{70} film observed at the laser-desorption power of 2.38 μJ per laser pulse. The spectrum was obtained without a matrix molecule such as cinapinic acid to assist the desorption and ionization. Thus, the peaks so obtained are free from H^+ adduct of the sample, though positive ions were detected in the actual measurements.

mm in diameter. Raman measurements were performed in a back-scattering geometry at room temperature using a JOBIN YBON T64000 triple monochromator equipped with a two-dimensional CCD detector operated at liquid-nitrogen temperature.

Calculations

Dimers of C_{70} were calculated using the MNDO Hamiltonian[24] with the AM-1 and PM-3 parametrizations[25] as implemented in the MOPAC program system.[26] For ease of direct comparison with literature data,[13,16] version 5.01 was used in this study. Symmetry constraints were not specified for the geometry optimization procedure, and the SCF convergence criteria were set at 10^{-8} kcal/mol.

A conventional [2+2]cycloaddition reaction[27] of C_{70} molecules was considered to be the initial stage of cross-linking, based on the theoretical results for C_{60} dimers.[13,16] Calculations were limited to the dimer structures of C_{70} having symmetries higher than C_{2v} and C_{2h}. Prior to the MO calculations, structures of the C_{70} dimers were optimized using molecular mechanics (MM) calculations.[28]

Results

Figure 1 shows the LDITOF-MS of the C_{70} polymer film observed at laser power of 2.38 μJ. At the same laser power, LDITOF-MS of an evaporated C_{70} film showed that the proportion of dimer to monomer was less than 1:60. Thus, Figure 1 confirms the plasma polymerization of C_{70} molecules by Ar plasma irradiation prior to the measurements, rather than by photoirradiation during LDITOF-MS observation. It can be seen in Figure 1 that the maximum mass values of the polymer peaks do not coincide with multiples of the initial mass of C_{70}. For example, the fifth peak was observed at about 4000 Da, which does not correspond to the mass of $(C_{70})_5$ (MW = 4204). Thus, direct cross-linking of C_{70} molecules must be accompanied by the loss of carbon atoms during plasma polymerization. This was confirmed by measuring the LDITOF-MS of the plasma-polymerized samples in the monomer and dimer mass regions at a slightly reduced laser power.

Figure 2a, b, and c shows the peak profiles of the monomer and dimer mass region of the C_{70} polymer film. The monomer envelope is composed of peaks associated with C_{70}, C_{68}, C_{66}, C_{64}, C_{62}, C_{60}, and C_{58} showing the C_2 loss during plasma irradiation. The dimer profile shown in Figure 2b is composed of strong peaks corresponding to $(C_{70})_2$, $(C_{70})_2 - (C_2)_n$ (n = 1−5), and very weak peaks corresponding to $(C_{70})_2 + (C_2)_n$ (n = 1−2). The higher peaks are C_{136} and C_{134}, and the peak of $(C_{70})_2$ is low. This peak profile closely resembles that of photopolymerized C_{60}[5,6] and that of plasma-polymerized C_{60}.[16] Figure 2c shows the LDITOF-MS of a C_{70} polymer generated under reduced plasma power at 25 W. The highest peak is C_{136} in this case, and the spectrum suggests that the degree of $(C_2)_n$ loss is dependent on the plasma power.

Raman spectra of the plasma-polymerized C_{60} and C_{70} films are shown in Figure 3, a and b, respectively. The films are photoemissive as can be seen in the spectra, though the emission is weak at ambient temperature. Raman shifts attributable to intact C_{60} and C_{70} cages were scarcely observed in the spectra. However, it is clear that the amount of intact cages remaining in the plasma-polymerized films is higher for C_{70} than for C_{60}. The spectral profile suggests that the plasma-polymerized C_{70} film is a carbon film with sp^2 carbons since the graphitic band appeared at 1570 cm^{-1}. A disordered band due to amorphous carbon, which usually appears at 1350 cm^{-1}, was scarcely observed in this case. X-ray diffraction measurements of the C_{70} polymer film formed on a glass substrate 300 nm in thickness showed no diffraction pattern, suggesting the lack of periodic crystal structure in the film.

The electric dark current of the C_{70} polymer formed on an Au-comb electrode was about 10^{-13} S/cm, indicating that the C_{70} polymer was almost insulating. Scanning electron microscope images of the plasma-polymerized C_{70} showed a hemispheric morphology, as observed for the plasma-polymerized C_{60}.[13] Finally, electron spin resonance measurement of the plasma-polymerized C_{70} film showed that the number of dangling bonds remained on the same level as found for plasma-polymerized C_{60} film.[13]

Discussion

Our examination of the structure of C_{60} dimers having dumbbell shapes with intact C_{60} cages formed by 1,2-, 1,4-, and 1,2+1,4-cycloaddition of a cyclohexatrienyl unit to each of the C_{60} molecules suggested that the 1,2-cycloaddition reaction led to the most stable dimer.[14] Initially, the theoretical examination of C_{70} dimers produced by plasma polymerization was limited to those formed by the [2+2]cycloaddition reaction. Figure 4 shows the optimized structure of C_{70} and the numbering system adopted in this work. The 105 C−C bonds in a C_{70} molecule having D_{5h} symmetry can be classified into eight types, as shown in Table 1. The C−C bonds between two adjacent hexagons are double bond in nature except for the C(11)−C(12) bond, which seems to be a single bond. It is noteworthy that the bond length and bond order of the C(9)−C(10) bond are double-bond-like, although the bond participates in the formation of a pentagon. We chose the C(2)−C(4), C(5)−C(6), C(9)−C(10), C(10)−C(11), and C(11)−C(12) bonds to examine [2+2]-cycloaddition of the C_{70} molecules. The C(11)−C(12) bond is included in the examination since this bond is 6,6-ring fusion. Twenty-five structures of C_{70} dimers are possible by [2+2]-cycloaddition of these bonds, among which only nine C_{70} dimers formed by [2+2]cycloaddition of identical bonds of two C_{70} molecules were examined.

The cycloaddition of C(2)−C(4), C(5)−C(6), C(9)−C(10), and C(10)−C(11) bonds leads to structural isomers, while that

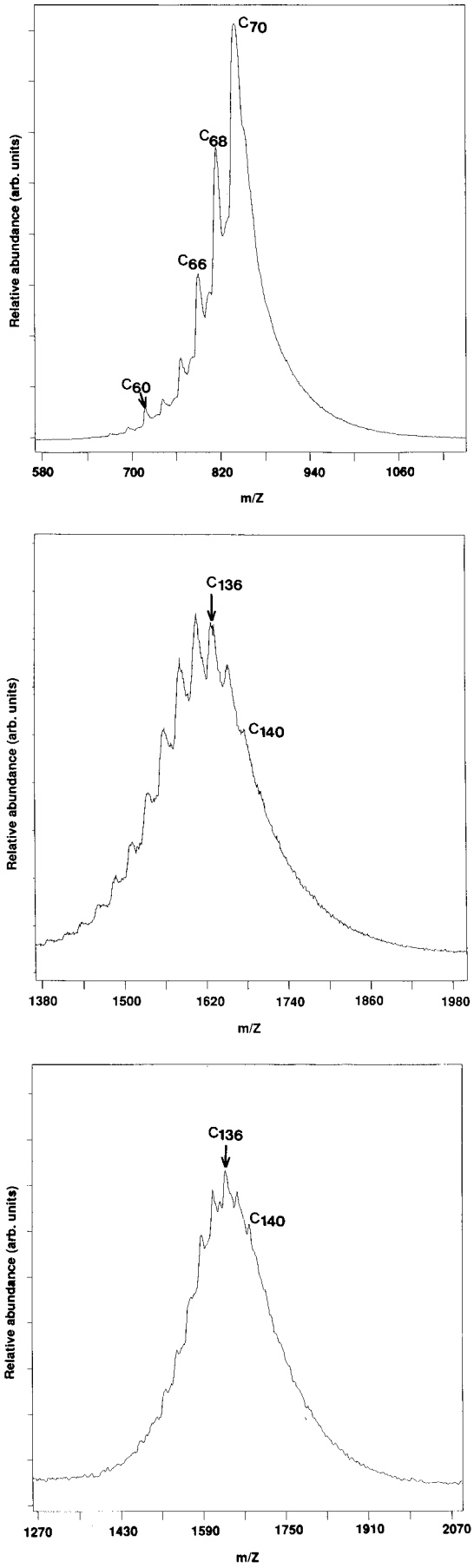

Figure 2. LDITOF-MS of the monomer (top) and dimer (middle) mass range observed at lower laser-desorption power of 1.20 μJ per laser pulse repeated 50 times. The bottom spectrum is dimer mass range observed on the C_{70} polymer film prepared at a plasma power of 25 W.

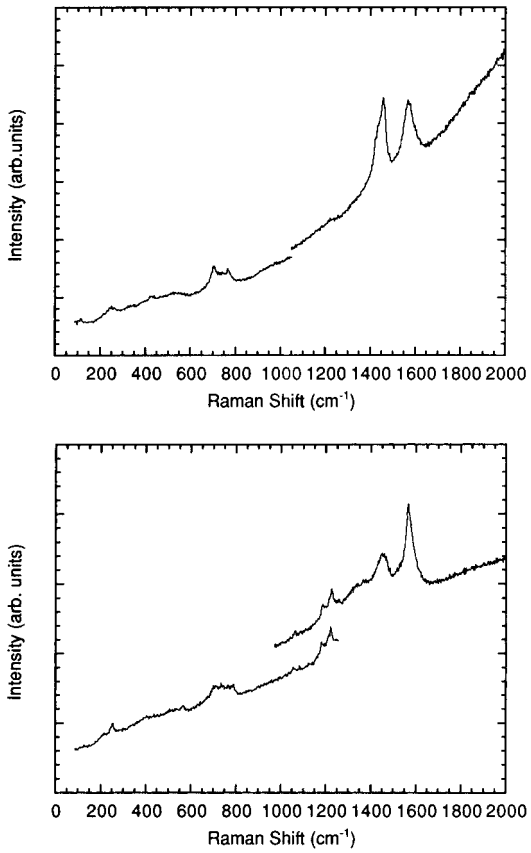

Figure 3. Raman spectra of the plasma-polymerized C_{60} (top) and C_{70} films (bottom). The 514.5 nm line from the Ar^+ laser was used for excitation.

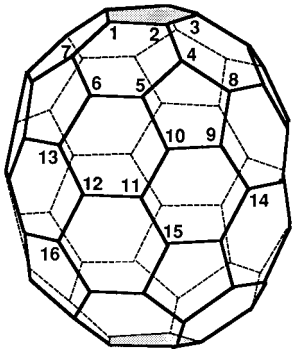

Figure 4. Optimized C_{70} structure and the numbering system adopted.

TABLE 1: Optimized C−C Bond Lengths and Bond Orders of C_{70} at MNDO/AM-1 Level[a]

bond[b]	bond length/Å	bond order
C(1)−C(2)	1.464	1.105
C(2)−C(4)	1.387	1.480
C(4)−C(5)	1.461	1.109
C(5)−C(6)	1.375	1.526
C(5)−C(10)	1.467	1.065
C(9)−C(10)	1.434	1.302
C(10)−C(11)	1.414	1.306
C(11)−C(12)	1.465	1.094

[a] The two types of C−C bond lengths in C_{60} molecule were calculated as 1.385 and 1.464 Å, and bond orders were calculated as 1.495 and 1.101 for each bond, respectively. [b] Numbering system adopted is shown in Figure 4.

of C(11)−C(12) bonds results in a structure with D_{2h} symmetry. The heats of reaction ($\Delta H_f°(r)$) in the formation of C_{70} dimers are listed in Table 2. The difference in kinetic energy between the anti-syn isomers is negligible for all pairs formed by cycloaddition of C(2)−C(4), C(5)−C(6), C(9)−C(10), and

TABLE 2: MNDO Heats of Reaction ($\Delta H°$(r)) in the Formation of C_{70} Dimers with Cyclobutane Ring

cluster	$\Delta H_f°$(r)[a] (kcal/mol)	$\Delta H_f°$(r)[b] (kcal/mol)	cross-link[c]	length[d] (Å)
C_{140}(a)	−34.63	−38.01	C(2)−C(2′), C(4)−C(4′)	1.544
			C(2)−C(4), C(2′)−C(4′)	1.607
C_{140}(b)	−34.33	−38.00	C(2)−C(4′), C(4)−C(2′)	1.544
			C(2)−C(4), C(2′)−C(4′)	1.607
C_{140}(c)	−33.94	−38.12	C(5)−C(5′), C(6)−C(6′)	1.550
			C(5)−C(6), C(5′)−C(6′)	1.613
C_{140}(d)	−33.92	−38.08	C(5)−C(6′), C(6)−C(5′)	1.551
			C(5)−C(6), C(5′)−C(6′)	1.624
C_{140}(e)	−19.05	−20.28	C(9)−C(9′), C(10)−C(10′)	1.553
			C(9)−C(10), C(9′)−C(10′)	1.655
C_{140}(f)	−18.54	−19.72	C(9)−C(10′), C(10)−C(9′)	1.555
			C(9)−C(10), C(9′)−C(10′)	1.655
C_{140}(g)	+3.19	−3.72	C(10)−C(10′), C(11)−C(11′)	1.559
			C(10)−C(11), C(10′)−C(11′)	1.613
C_{140}(h)	+3.27	−3.23	C(10)−C(11′), C(11)−C(10′)	1.560
			C(10)−C(11), C(10′)−C(11′)	1.613
C_{140}(i)	+64.30	+56.38	C(11)−C(11′), C(12)−C(12′)	1.560
			C(11)−C(12), C(11′)−C(12′)	1.683

[a] MNDO/AM-1 heat of reaction. [b] MNDO/PM-3 heat of reaction. [c] Numbering system is same as shown in Figure 4. The carbons represented as n' are those of the neighbor C_{70} in the same manner. [d] C−C bond lengths of pivot bonds forming cyclobutane rings predicted at the MNDO/AM-1 level. At the same level, the C−C bond lengths of ethane, benzene, and ethylene are calculated to be 1.500, 1.395, and 1.326 Å, respectively.

C(10)−C(11) bonds. The $\Delta H°$(r) values of the C_{70} dimers reveal that the stable dimers are derived from the [2+2]-cycloaddition of the C(2)−C(4) bonds and C(5)−C(6) bonds of C_{70} molecules. The $\Delta H°$(r) values of the formation of C_{140}-(a), C_{140}(b), C_{140}(c), and C_{140}(d) are very similar to that of the C_{60} dimer,[13,16] suggesting that the chemical nature of the C(2)−C(4) and C(5)−C(6) bonds of the C_{70} molecule is almost the same as that of weakly conjugated C−C double bonds in the C_{60} molecule. In these four C_{140} structures, the bond alternations of the C_{70} moieties are scarcely changed, as in the case of C_{60} dimer by [2+2]cycloaddition.[16]

The structures C_{140}(e) and C_{140}(f) are destabilized by 15 and 18 kcal/mol at the AM-1 and PM-3 levels, respectively, compared to the structures C_{140}(a), C_{140}(b), C_{140}(c), and C_{140}-(d). The isomers of C_{140}(g) and C_{140}(h) were found to be endothermic at the AM-1 level only, whereas the C_{140}(i) is strongly destabilized. The $\Delta H°$(r) values of the C_{70} dimer formed by cycloaddition of the C(1)−C(2) bonds, whose pivot bonds are C(1)−C(2′) and C(1′)−C(2), are +0.19 and −1.88 kcal/mol at AM-1 and PM-3 levels, respectively. These values are very similar to those of the formation of C_{140}(g) and C_{140}-(h). Thus, the [2+2]cycloaddition reaction of C_{70} molecules can only occur at the C(2)−C(4), C(5)−C(6), and C(9)−C(10) bonds and the probability of the reaction of the C(9)−C(10) bonds is lower than those of the C(2)−C(4) bonds and C(5)−C(6) bonds. The cycloaddition of C(10)−C(11) and C(11)−C(12) bonds should be dynamically impossible.

To clarify the contribution of the steric strain to $\Delta H°$(r) brought about by the overlapping $2p^z$ lobes of carbon atoms adjacent to the cross-link bonds in the formation of C_{140}(a)−C_{140}(i), [2+2]cycloaddition of C_{70} and C_{60} molecules and hydrogenation of C_{70} were theoretically examined. Table 3 shows the $\Delta H_f°$ values in the formation of C_{70} dimers and C_{70}−C_{60} structures by [2+2]cycloaddition, together with the values in the formation of $C_{70}H_2$. In Table 3, all $\Delta H_f°$ values are reported relative to that of the C_{70} dimer cross-linked at the C(5) and C(6) atoms, since the MNDO/PM-3 $\Delta H_f°$ value for the C_{140}(c) is the smallest among those of C_{70} dimers shown in Table 2. In the case of the C_{70}−C_{60} and $C_{70}H_2$ structures, the difference in $\Delta H_f°$ values depends on the change in the electronic structure of the C_{70} moiety brought about by the addition reaction. It can clearly be seen in Table 3 that the difference of the $\Delta H_f°$ values in the formation of C_{70} dimers is almost twice as large as that found for the formation of the C_{70}−C_{60} and $C_{70}H_2$ structures. This suggests that the formation of the C_{70} dimers is scarcely affected by the overlapping of the $2p^z$ lobes of carbon atoms adjacent to the cross-link bonds. Instead, only the structural strain in the cyclobutane rings and the changes in the electronic structure of the C_{70} moieties contribute to the $\Delta H_f°$ values of C_{70} dimers, within the framework of MNDO approximation.

TABLE 3: Relative MNDO Heats of Formation ($\Delta H_f°$) in the formation of C_{70} Dimers and C_{70}−C_{60} Adducts Derived from [2+2]Cycloaddition, and Those in the Formation of $C_{70}H_2$ (in kcal/mol)

	2(C_{70})		C_{70}−C_{60}		$C_{70}H_2$	
form[a]	AM-1	PM-3	AM-1	PM-3	AM-1	PM-3
C(2), C(4)	−0.69	+0.11	+2.21	+2.46	+1.03	+1.07
	−0.66	+0.12				
C(5), C(6)[b]	0	0	0	0	0	0
	+0.02	+0.04				
C(9), C(10)	+14.89	+17.84	+7.64	+8.89	+6.88	+7.07
	+15.40	+18.40				
C(10), C(11)	+37.13	+34.40	+18.57	+17.59	+19.88	+18.30
	+37.21	+34.89				
C(11), C(12)	+98.24	+94.50	+50.49	+48.33	+51.77	+48.45

[a] Carbon atoms forming cyclobutane rings in C_{70} dimers and C_{70}−C_{60} adducts, and those connected with H atoms in $C_{70}H_2$. [b] $\Delta H_f°$ values are chosen as zero reference.

As is shown in Figure 2, the cross-linking of C_{70} molecules is accompanied by C_2 loss. Therefore, in order to investigate the direct cross-linking of C_{70} molecules in further detail, C_{136} molecules were theoretically examined. The C_{136} molecules examined were constructed as follows: the four carbon atoms participating in the formation of the cyclobutane rings in the C_{140}(a)−C_{140}(i) molecules are eliminated, and the two C_{68} moieties with four dangling bonds are recombined. The optimized structures of C_{136} are shown in Figure 5, and the calculated results are collected in Table 4. In this table, the $\Delta H_f°$ values for C_{136}(c) are chosen as zero reference in order to compare the degree of stability of these C_{136} molecules. The $\Delta H_f°$ values suggest that C_{136}(a) and C_{136}(b) are effectively stabilized by this type of cross-linking. On the other hand, C_{136}-(e), C_{136}(f), and C_{136}(i) are destabilized. The stability of C_{136}-(d), C_{136}(g), and C_{136}(h) is similar to that of C_{136}(c). Among these C_{136} structures, only C_{136}(a) and C_{136}(b) disturb to a small extent the electronic structure of the intact C_{70} molecule.

[2+2]Cycloaddition should be an initial process of direct cross-linking of C_{60} molecules, and C_2 loss occurs in the C_{60} dimer.[16] A possible mechanistic pathway of C_2 loss is schematically shown in Figure 6 for the structure C_{140}(a). As shown in Table 2, the C(2)−C(2′) crosslink bond of C_{140}(a) is 1.544 Å, and the C(2)−C(4) bond forming the cyclobutane ring is 1.607 Å. This suggests that highly strained C−C bonds exist in the C(2)−C(4) bond. If scission of these highly strained C(2)−C(4) and C(2′)−C(4′) bonds occurs, the C_{140}(a) is free from sp^3 carbon atoms, (Figure 6b). This C_{70} dimer with only sp^2 carbon atoms, however, is less stable than the initial dimer formed by [2+2]cycloaddition, as seen in the dimerization of C_{60}.[16] The structure shown in Figure 6b is therefore stabilized by rearrangement without C_2 loss, as shown by Scuseria et al.[29] and Osawa[30] in the case of the C_{60} dimer. This Stone−Wales rearrangement[31] results in the formation of a dimer having ladder-shaped crosslinks, (Figures 6c and d). By elimination of two carbon atoms forming one of the ladder-shaped cross-links in structure 6c, the C_{138} shown in Figure 6e can be derived. Further elimination of C_2 and recombination of the dangling bonds finally results in the formation of C_{136}(a) (Figure 6f).

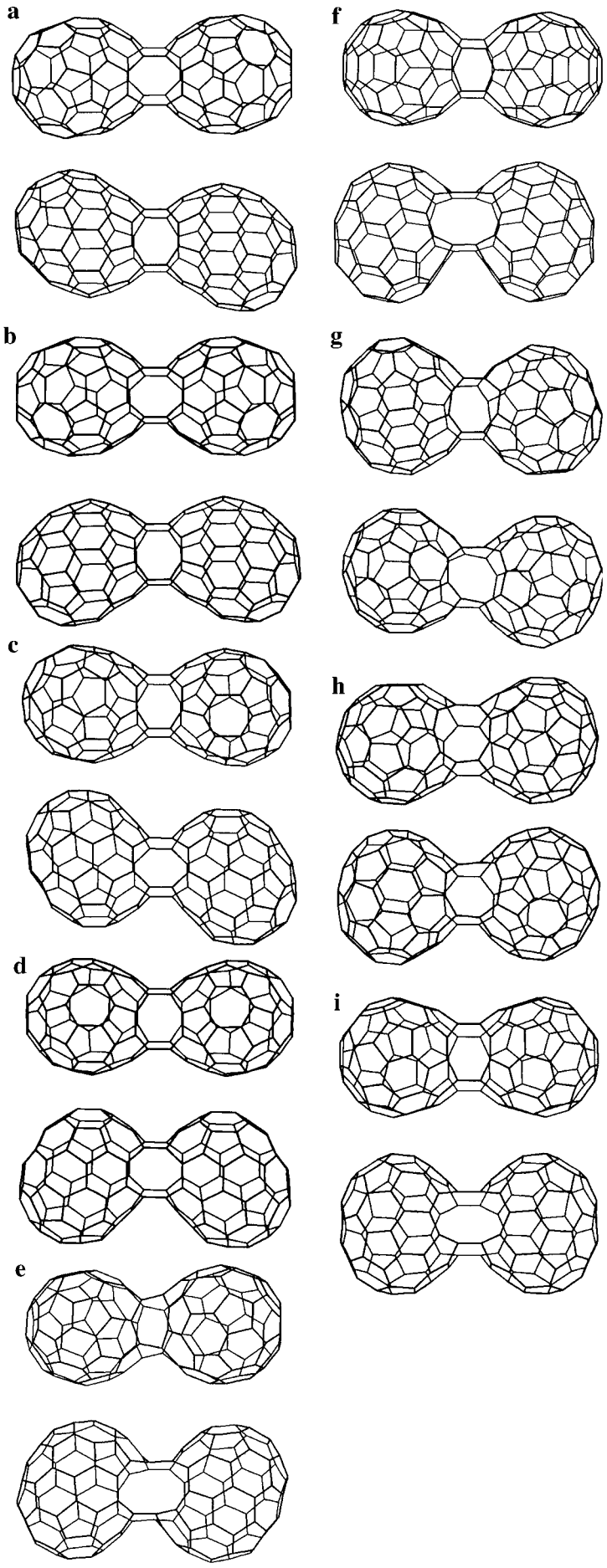

Figure 5. Optimized structures of C_{136} derived from the corresponding C_{70} dimers by elimination of four carbon atoms forming cyclobutane rings and recombination of C_{68} moieties.

TABLE 4: Relative MNDO Heats of Formation ($\Delta H_f°$) for C_{136} Molecules Derived from Corresponding C_{140} Molecules in Table 2

cluster[a]	$\Delta H_f°$ [b] (kcal/mol)	$\Delta H_f°$ [c] (kcal/mol)	cross-link[d]	length (Å)
C_{136}(a)	−65.50	−61.60	C(1)−C(8′), C(3)−C(5′)	1.351
			C(5)−C(3′), C(8)−C(1′)	1.351
C_{136}(b)	−64.44	−61.54	C(1)−C(3′), C(3)−C(1′)	1.351
			C(5)−C(8′), C(8)−C(5′)	1.351
C_{136}(c)	0	0	C(4)−C(13′), C(7)−C(10′)	1.352
			C(10)−C(7′), C(13)−C(4′)	1.352
C_{136}(d)	+0.09	+0.11	C(4)−C(7′), C(7)−C(4′)	1.351
			C(10)−C(13′), C(13)−C(10′)	1.354
C_{136}(e)	+112.98	+102.89	C(5)−C(8′), C(8)−C(5′)	1.353
			C(11)−C(14′), C(14)−C(11′)	1.372
C_{136}(f)	+69.47	+59.44	C(5)−C(14′), C(14)−C(5′)	1.358
			C(11)−C(8′), C(8)−C(11′)	1.352
C_{136}(g)	−3.74	−9.20	C(5)−C(15′), C(15)−C(5′)	1.344
			C(12)−C(9′), C(9)−C(12′)	1.352
C_{136}(h)	+2.82	−5.30	C(5)−C(9′), C(9)−C(5′)	1.372
			C(12)−C(15′), C(15)−C(12′)	1.334
C_{136}(i)	+98.50	+84.36	C(13)−C(10′), C(15)−C(16′)	1.376
			C(10)−C(13′), C(16)−C(15′)	1.376

[a] $\Delta H_f°$ values for the structure c are chosen as zero reference. [b] MNDO/AM-1 heat of formation. [c] MNDO/PM-3 heat of formation. [d] Four pivot bonds in C_{136} clusters.

$\Delta H_f°$ values per carbon atom for the above-discussed C_{140} and C_{136} structures are reported in Table 5. At present, we have no clear explanation for the C_2 loss from a highly excited C_{70} molecule as reported in the case of C_{60}.[32,33] However, from Table 5 it can be seen that the process shown in Figure 6 constitutes a plausible process of structural relaxation of initially formed C_{70} dimer. Recently, Osawa showed that a C_{120} having a one-dimensional tubular shape can be obtained by the Stone−Wales rearrangement from the initial C_{60} dimer,[30] while the C_2 loss occurs prior to the type of structural relaxation in the case of plasma polymerization of C_{60} and C_{70}. Not only the C_2 loss but also the addition of C_2 fragments with the C_{70} polymer is stimulated in the course of plasma polymerization of C_{70}. Just as the radical addition reported by Krusic et al.[34,35] and McEwen et al.,[36] the highly active C_2 fragment should be added to the weakly conjugated double bonds of the C_{70} molecule or its polymer in the course of plasma polymerization, forming a cyclobutene structure.

TABLE 5: MNDO Heats of Formation ($\Delta H_f°$) per Carbon Atom for C_{140} and C_{136} Molecules

cluster	$\Delta H_f°$/C[a] (kcal/mol)	$\Delta H_f°$/C[b] (kcal/mol)	cluster	$\Delta H_f°$/C[a] (kcal/mol)	$\Delta H_f°$/C[b] (kcal/mol)
C_{70}	15.171	12.631			
C_{140}(a)	14.924	12.359	C_{136}(a)	14.643	12.295
C_{140}(b)	14.924	12.360	C_{136}(b)	14.643	12.295
C_{140}(c)	14.929	12.359	C_{136}(c)	15.117	12.748
C_{140}(d)	14.929	12.359	C_{136}(d)	15.118	12.748
C_{140}(e)	15.035	12.486	C_{136}(e)	15.947	13.546
C_{140}(f)	15.039	12.490	C_{136}(f)	15.627	13.252
C_{140}(g)	15.194	12.607	C_{136}(g)	15.090	12.680
C_{140}(h)	15.194	12.608	C_{136}(h)	15.138	12.709
C_{140}(i)	15.630	13.034	C_{136}(i)	15.841	13.368

[a] MNDO/AM-1 heat of formation per carbon atom. [b] MNDO/PM-3 heat of formation per carbon atom.

In the above discussion, it was suggested that C_{70} is less reactive than C_{60} toward cycloaddition reaction. To confirm the lower probability of a direct cross-linking of C_{70} molecules, the efficiency of photopolymerization of C_{60}, a 1:1 mixture of C_{60}/C_{70}, and C_{70} was examined using a reflectron type LDITOF-MS monitor. In the observations, the fine crystals of these samples were set on the ionization target and ionized directly by N_2 laser irradiation. The laser power was increased sufficiently to cause photo-polymerization. Figure 7, a, b, and c shows the mass profiles of photopolymerized C_{60}, a C_{60}/C_{70} mixture, and C_{70}, respectively. In this type of photopolymerization, the probability of a direct cross-linking depends on the molecular orientation at the moment of pulse laser irradiation whose pulse width is about 5 ns. As can be seen in Figure 7,

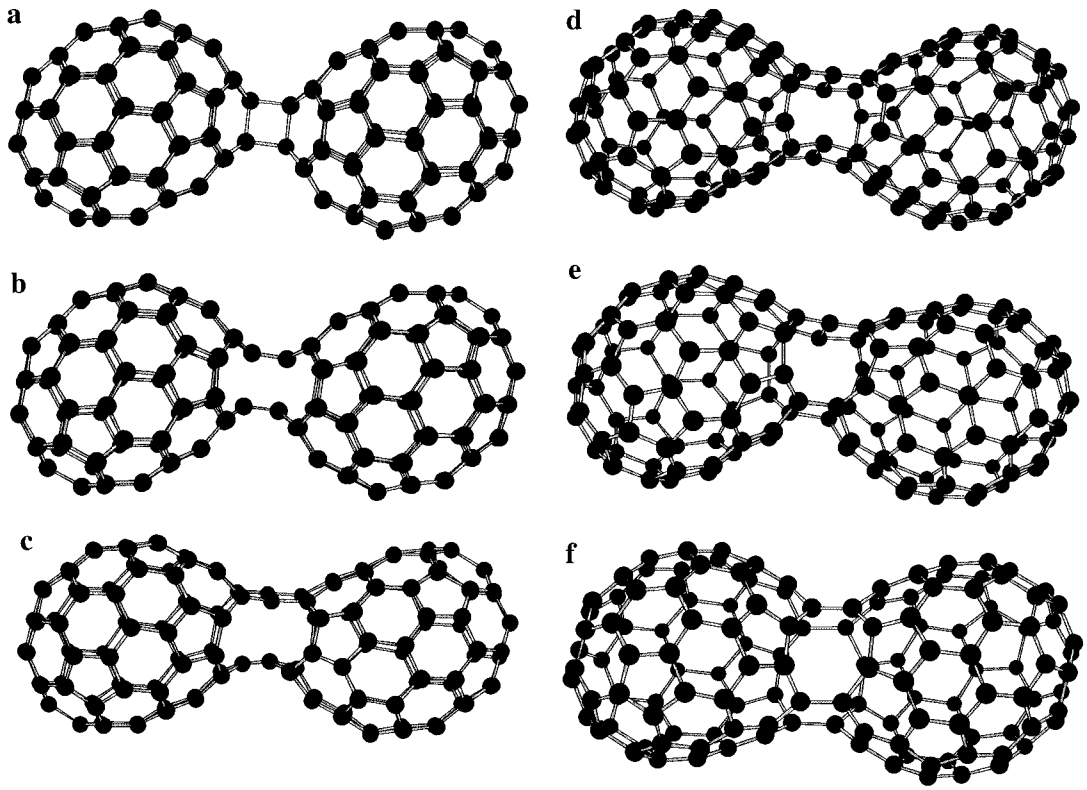

Figure 6. (a) The C_{70} dimer corresponds to C_{140}(a) in Figure 4. (b) C_{140} is derived from the scission of highly strained bonds forming cyclobutane. (c) C_{140} is derived from structure b by the Stone−Wales rearrangement. (d) C_{140} is derived from structure c by further structural rearrangement of the cross-link bond. (e) C_{138} is derived from structure d by C_2 loss and recombination of dangling bonds. (f) C_{136} is derived from structure d by further C_2 loss and recombination of dangling bonds.

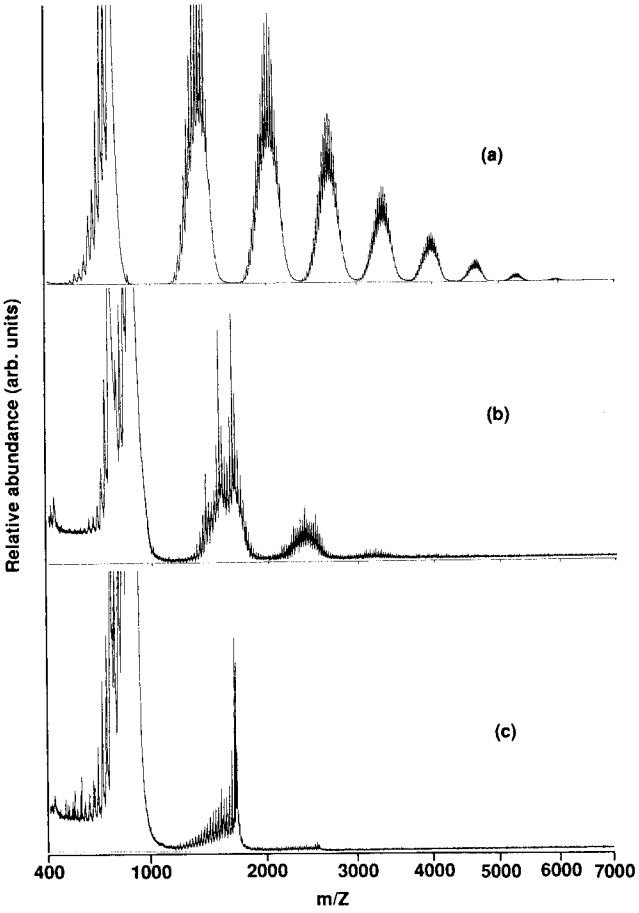

Figure 7. LDITOF-MS of C_{60} (a, top), a 1:1 mixture of C_{60}/C_{70} (b, middle), and C_{70} (c, bottom) observed using a reflectron-type ion monitor.

at the same laser power the degree of polymerization of C_{70} is obviously less than those of C_{60} and the C_{60}/C_{70} mixture.

The value of the electric dark current of the plasma-polymerized C_{70} film was found to be smaller by 5 orders of magnitude than that of the C_{60} films obtained at the same plasma power. Based on the above discussion, the insulator-like electric conductivity of the plasma-polymerized C_{70} film can be attributed to a lower number of direct cross-links of C_{70} molecules. The cross-link bonds, as shown in Figure 5, allow electron migration between the fullerene cages through π-conjugation, but the cross-link bonds in the sp^3 valence state formed by [2+2]-cycloaddition are likely to suppress the electron migration between C_{70} cages. Electron migration between the C_{70} residues is impossible in an open-shell C_{70} dimer having a cross-link bond, which has two unpaired electrons at the carbon atoms adjacent to the cross-link bond. The C_{70} molecules which occasionally remain intact in plasma-polymerized film are responsible for the very low electric conductivity.

It follows that the direct cross-links in the plasma-polymerized C_{70} films can be classified into two types according to their cross-link structure. One type is characterized by conductive bonds formed by C_2 loss and successive recombination resulting in π-conjugation. The other type contains insulating bonds such as found in C_{70} dimers derived from [2+2]cycloaddition, or in open-shell C_{70} dimer having only one cross-link bond. These two types of cross-links are interrelated in the polymer films in the sense that when the number of one type is high, the other is correspondingly low. The electric conductivity of the plasma-polymerized C_{60} and C_{70} films could change drastically at a certain level of formation of conducting cross-link bonds, that is, at the percolation limit.

Concluding Remarks

LDITOF mass analysis of plasma-polymerized C_{70} films suggests that direct cross-linking of C_{70} molecules under Ar plasma is accompanied by C_2 loss, as in the case of C_{60}.[16] MO calculations of C_{70} dimer structures suggest that a direct cross-linking occurs at the double bonds in the polyhedral caps rather than the graphitic belt of the C_{70} molecule. The calculations also suggest that the polyhedral caps of the C_{70} molecule are almost identical in chemical properties with the C_{60} molecule. Furthermore, MO study of plausible C_{136} molecules formed by elimination of four carbon atoms from the cyclobutane ring in the C_{70} dimer suggests that the C_{136} molecules derived from stable initial C_{70} dimers are more stable than those derived from the unstable C_{70} dimers.

The almost insulating electric conductivity of the plasma-polymerized C_{70} films is attributed to a lower probability of conductive cross-linking than that of C_{60}. Taking into account the fact that the C_{70} molecule has a graphitic belt which is less reactive than the polyhedral caps toward the addition reaction, the C_{70} molecule can be regarded as structurally possible and as the smallest carbon nanotube, as well as a ellipsoidal fullerene with 70 carbon atoms.

Acknowledgment. The authors thank Professor Dr. E. Osawa (Toyohashi University of Technology), Dr. K. Harigaya (Electrotechnical Laboratory), Mr. P. Strasser, Dr. J. Westwater, Dr. N. Kishii, and Mr. Y. Gonno (Sony Research Center) for their fruitful discussions and help. This research is contracted with Research Institute of Innovative Technology for the Earth (RITE).

References and Notes

(1) Kroto, H. W.; Heath, J. R.; O'Brien, S. C.; Curl, R. F.; Smalley, R. E. *Nature* **1985**, *318*, 162.

(2) (a) Krätschmer, W.; Fostiropoulos, K.; Huffman, D. R. *Chem. Phys. Lett.* **1990**, *170*, 167. (b) Krätschmer, W.; Lamb, L. D.; Fostiropoulos, K.; Huffman, D. R. *Nature* **1990**, *347*, 354.

(3) (a) Rao, A. M.; Zhou, P.; Wang, K.-A.; Hager, G. T.; Holden, J. M.; Wang, Y.; Lee, W.-T.; Bi, X.-X.; Eklund, P. C.; Cornett, D. S.; Duncan, M. A.; Amster, I. J. *Science* **1993**, *259*, 955. (b) Cornett, D. C.; Amster, I. J.; Duncan, M. A.; Rao, A. M.; Eklund, P. C. *J. Phys. Chem.* **1993**, *97*, 5036.

(4) Zhou, P.; Dong, Z.-H.; Rao, A. M.; Eklund, P. C. *Chem. Phys. Lett.* **1993**, *211*, 337.

(5) Wang, Y.; Holden, J. M.; Dong, Z.-H.; Bi, X.-X.; Eklund, P. C. *Chem. Phys. Lett.* **1993**, *211*, 341.

(6) Ito, A.; Morikawa, T.; Takahashi, T. *Chem. Phys. Lett.* **1993**, *211*, 333.

(7) Akselrod, L. A.; Byrne, H. J.; Thomsen, C.; Mittelbach, A.; Roth, S. *Chem. Phys. Lett.* **1993**, *212*, 384.

(8) McElvany, S. W.; Callahan, J. H.; Ross, M. M.; Lamb, L. D.; Huffman, D. R. *Science* **1993**, *260*, 1632.

(9) (a) Pekker, S.; Forró, L.; Mihàly, L.; Jánossy, A. *Solid State Commun.* **1994**, *90*, 349. (b) Stephens, P. W.; Bortel, G.; Faigel, G.; Tegze, M.; Jánossy, A.; Pekker, S.; Oszlányi, G.; Forró, L. *Nature* **1994**, *370*, 636. (c) Chauvet, O.; Oszlányi, G.; Folló, L.; Stephens, P. W.; Tegze, M.; Faigel, G.; Jánossy, A. *Phys. Rev. Lett.* **1994**, *72*, 2721. (d) Pekker, S.; Jánossy, A.; Mihaly, L.; Chauvet, O.; Carrard, M.; Forró, L. *Science* **1994**, *265*, 1077. (e) Martin, M. C.; Koller, D.; Rosenberg, A.; Kendziora, C.; Mihaly, L. *Phys. Rev. B* **1995**, *51*, 3210.

(10) Iwasa, Y.; Arima, T.; Freming, R. M.; Siegrist, T.; Zhou, O.; Haddon, R. C.; Rothberg, L. J.; Lyons, K. B.; Carter Jr., H. L.; Hebard, A. F.; Tycko, R.; Dabbagh, G.; Karajewski, J. J.; Thomas, G. A.; Yagi, T. *Science* **1994**, *264*, 1570.

(11) (a) Múñez-Regueiro, M.; Marques, L.; Hodeau, J. L.; Béthoux, O.; Perroux, M. *Phys. Rev. Lett.* **1995**, *74*, 278. (b) Oszlanyi, G.; Folló, L. *Solid State Commun.* **1995**, *93*, 265. (c) Harigaya, K. *Phys. Rev. B* **1995**, *52*, 7968. (d) Tanaka, K.; Matsuura, Y.; Oshima, Y.; Yamabe, T. *Solid State Commun.* **1995**, *93*, 163.

(12) Xu, C. H.; Scuseria, G. E. *Phys. Rev. Lett.* **1995**, *74*, 274.

(13) Takahashi, N.; Dock, H.; Matsuzawa, N.; Ata, M. *J. Appl. Phys.* **1993**, *74*, 5790.

(14) Matsuzawa, N.; Ata, M.; Dixon, D. A.; Fitzgerald, G. *J. Phys. Chem.* **1994**, *98*, 2555.

(15) (a) Menon, M.; Subbaswamy, K. R.; Sawtarie, M. *Phys. Rev.* **1994**, *B49*, 13966. (b) Taylor, R. *J. Chem. Soc., Chem. Commun.* **1994**, 1629.

(16) Ata, M.; Takahashi, N.; Nojima, K. *J. Phys. Chem*. **1994**, *98*, 9960.
(17) (a) Diederich, F.; Ettle, R.; Rubin, Y.; Whetten, R. L.; Beck, R.; Alvarez, M.; Anz, S.; Sensharma, D.; Wudl, F.; Khemani, K. C.; Koch, A. *Science* **1991**, *252*, 548. (b) Raghavachari, K.; Rohlfing, C. M. *Chem. Phys. Lett*. **1992**, *97*, 495. (c) Akasaka, T.; Mitsuhida, E.; Ando, W.; Kobayashi, K.; Nagase, S. *J. Am. Chem. Soc*. **1994**, *116*, 2627.
(18) (a) Balch, A. L.; Catalano, V. J.; Lee, J. W.; Olmstead, M. M.; Parkin, S. R. *J. Am. Chem. Soc*. **1991**, *113*, 8953. (b) Hawkins, J. M.; Meyer, A.; Solow, M. A. *J. Am. Chem. Soc*. **1993**, *115*, 7499.
(19) (a) Hirsch, A.; Grösser, T.; Skiebe, A.; Soi, A. *Chem. Ber*. **1993**, 126, 1061. (b) Bingel, C. *Chem. Ber*. **1993**, *126*, 1957. (c) Guldi, D. M.; Hungerbühler, H.; Wilhelm, M.; Asmus, K.-D. *J. Chem. Soc., Faraday Trans*. **1994**, *90*, 1391.
(20) (a) Borghi, R.; Lunazzi, L.; Placucci, G.; Krusic, P. J.; Dixon, D. A.; Knight, Jr. L. B. *J. Phys. Chem*. **1994**, *98*, 5395. (b) Morton, J. R.; Negri, F.; Preston, K. F. *Chem. Phys. Lett*. **1994**, *218*, 467. (c) Morton, J. R.; Preston, K. F.; Negri, F. *Chem. Phys. Lett*. **1994**, *221*, 59. (d) Henderson, C. C.; Rohlfing, C. M.; Gillen, K. T.; Cahill, A. A. *Science* **1994**, *264*, 397. (e) Cataldo, F. *Carbon* **1994**, *32*, 437.
(21) Rao, A. M.; Menon, M.; Wang, K.-A.; Eklund, P. C.; Subbaswamy, K. R.; Cornett, D. S.; Duncan, M. A.; Amster, I. J. *Chem. Phys. Lett*. **1994**, *224*, 106.
(22) (a) Hare, J. P.; Dennis, T. J. S.; Kroto, H. W.; Taylor, R.; Allaf, W. A.; Balm, S.; Walton, D. R. M. *J. Chem. Soc., Chem. Commun*. **1991**, 412. (b) Bethune, D. S.; Meijer, G.; Tang, W. C.; Rosen, H. J.; Golden, W. G.; Seki, H.; Brown, C. A.; de Vries, M. S. *Chem. Phys. Lett*. **1991**, *179*, 181. (c) Dennis, T. J. S.; Hare, J. P.; Kroto, H. W.; Tayler, R.; Walton, D. R. M.; Hendra, P. J. *Spectrochim. Acta* **1991**, *47A*, 1289. (d) Christides, C.; Nikolaev, A. V.; Dennis, T. J. S.; Prassides, K.; Negri, F.; Orlandi, G.; Zerbetto, F. *J. Phys. Chem*. **1993**, *97*, 3641. (e) Jishi, R. A.; Dresselhaus, M. S.; Dresselhaus, G.; Wang, K.-A.; Zhou, P.; Rao, A. M.; Eklund, P. C. *Chem. Phys. Lett*. **1993**, *206*, 187. (f) van Loosdrecht, P. H.; Verheijen, M. A.; Meekes, H.; van Bentum, P. J. M.; Meijer, G. *Phys. Rev. B* **1993**, *47*, 7610.
(23) Yoshikawa, M.; Nagai, N.; Matsuki, M.; Fukuda, H.; Katagiri, G.; Ishida, I.; Isitani, A.; Nagai, I. *Phys. Rev. B* **1992**, *46*, 7169.
(24) Stewart, J. J. P. *J. Comput.-Aided Mol. Des*. **1990**, *4*, 1.
(25) Dewar, M. J. S.; Zoebisch, E. G.; Healy, E. F.; Stewart, J. J. P. *J. Am. Chem. Soc*. **1985**, *107*, 3902.
(26) Stewart, J. J. P. QCPE Program 455, 1983; Version 5.10.
(27) (a) Wilson, S. R.; Kaprinidis, N.; Wu, Y.; Schuster, D. I. *J. Am. Chem. Soc*. **1993**, *115*, 8495. (b) Zhang, X.; Romero, A.; Foote, S. *J. Am. Chem. Soc*. **1993**, *115*, 11024.
(28) Locally developed software was kindly provided by Dr. N. Kishii of the Sony Corp. Res. Center.
(29) (a) Murry, R. L.; Strout, D. L.; W. C.; Odom, G. K.; Scuseria, G. E. *Nature* **1993**, *366*, 665. (b) Strout, D. L.; Murry, R. L.; Xu, C.; Eckhoff, W. C.; Odom, G. K.; Scuseria, G. E. *Chem. Phys. Lett*. **1993**, *214*, 576. (c) Eckhoff, W. C.; Scuseria, G. E. *Chem. Phys. Lett*. **1993**, *216*, 399.
(30) Osawa, E., private communication.
(31) (a) Stone, A. J.; Wales, D. J. *Chem. Phys. Lett*. **1986**, *128*, 501. (b) Saito, R. *Chem. Phys. Lett*. **1992**, *195*, 537. (c) Saito, R.; Dresselhaus, G. D.; Dresselhaus, M. S. *Chem. Phys. Lett*. **1992**, *195*, 537. (d) Osawa, S.; Osawa, E. *Fullerene Sci. Technol*. **1995**, *3*, 565.
(32) Fieber-Erdmann, M.; Krätschmer, W.; Ding, A. *Z. Phys. D* **1993**, *26*, 308.
(33) Petrie, S.; Bohme, D. K. *Nature* **1993**, *356*, 426.
(34) (a) Krusic, P. J.; Wasserman, E.; Parkinson, B. A.; Malone, B.; Holler, E. R.; Keizer, P. N.; Morton, J. R.; Preston, K. F. *J. Am. Chem. Soc*. **1991**, *113*, 6274. (b) Morton, J. R.; Preston, K. F.; Krusic, P. J.; Hill, S. A.; Wasserman, E. *J. Phys. Chem*. **1992**, *96*, 3576. (c) Keizer, P. N.; Morton, J. R.; Preston, K. F. *J. Chem. Soc., Chem. Commun*. **1992**, 1259.
(35) (a) Krusic, P. J.; Wasserman, E.; Keizer, P. N.; Morton, J. R.; Preston, K. F. *Science* **1991**, *254*, 1183. (b) Morton, J. R.; Preston, K. F.; Krusic, P. J.; Hill, S. A.; Wasserman, E. *J. Am. Chem. Soc*. **1992**, *114*, 5454.
(36) McEwen, C. N.; McKay, R. G.; Larsen, B. S. *J. Am. Chem. Soc.* **1992**, *114*, 4412.